Sample Preparation for Single-Electron Spin Detection

CNF Project Number: 863-00

Principal Investigator(s): John A. Marohn

User(s): Peter (Hanyu) Sun

Affiliation(s): Department of Chemistry and Chemical Biology, Cornell University

Primary Source(s) of Research Funding: Army Research Office

Contact: jam99@cornell.edu, hs859@cornell.edu

Website: marohn.chem.cornell.edu

Primary CNF Tools Used: CVC SC4500 e-gun evaporation system

Abstract:

Magnetic resonance force microscopy (MRFM) is a scanning probe microscopy technique that aims to achieve high force sensitivity and sub-nanometer resolution of magnetic spins through spatially resolved magnetic resonance. This report discusses a recent study on methods of preparing MRFM samples at the Cornell NanoScale Science and Technology Facility (CNF) that will improve sample preparation techniques and progress us towards the goal of single electron detection and imaging in an MRFM microscope.

Summary of Research:

In MRFM, nuclear magnetic resonance or electron spin resonance are detected as a force or force gradient on the tip of a microscopic cantilever. The Marohn group prepares attonewton-sensitivity nanomagnet-tipped cantilevers using a method previously developed at the CNF.

In recent test experiments, the sample is a 200 nm thick layer of polystyrene doped with an electron radical spin probe, 4-amino-TEMPO. This polystyrene sample is spin-coated on a coplanar waveguide (10 mm by 2 mm by 0.5 mm). A 12 nm gold film is then deposited on top of the polystyrene by electron-beam vapor deposition and wire-bonded to the ground plane.

It has been shown that with the gold film, surface non-contact friction from the sample can be sufficiently reduced to achieve signal to noise ratio necessary for single electron detection. However, comparing recent measurements of them MRFM-ESR signal to numerical simulations suggests the existence of a 20 nm layer at the top of the sample in which the 4-amino-TEMPO does not contribute to the signal.

Bulk ESR measurements suggest the reduction in signal may be due to sample damage induced by e-beam vapor deposition of the gold layer.

In this study we investigated an alternative hypothesis, that magnetic field fluctuations from the metal film reduced the spin-lattice relaxation time T1 of electron radical spins to a degree that made them undetectable via MRFM.

Thermal motion of electrons in materials produce small magnetic fields. Near the surface of conductive materials such as metals, these charge fluctuations can produce enough magnetic field fluctuations at the electron Larmor frequency to produce electron relaxation. In their 2018 paper, Ariyaratne, et al., develop equations to quantify this relaxation effect and use the T1 relaxation of nitrogen-vacancy (NV) centers as a detector of conductivity in metal films (85 nm thick Ti, Al and Ag films) [1]. The induced relaxation rate is proportional to the conductivity of the metal thin film and related to the distance between the targeted spin and the metal film.

The work done at the CNF allows us to predict the effect of our 12 nm gold film on the MRFM sample. The test sample was a 200 nm polystyrene film spin-coated on a silicon chip identical in size to our coplanar waveguide. A 12 nm gold film was deposited on top of the polystyrene film with the CVC SC4500 e-gun evaporation system at the CNF. The resulting samples were wired bonded and the resistivity of the gold film was measured using Quantum Design 14T "Blue" Physical Property Measurement System (PPMS) at the Cornell Center for Materials Research (CCMR). The resistivity was profiled at 4.2 K and 10^{-5} Torr, conditions closely resembling MRFM operating conditions. The preliminary data shows a resistivity of 116 nΩ-m for the 12 nm gold film on polymer, suggesting that the relaxation rate of electron spins in the polystyrene sample due to the gold film would be minimal.

We expect to further explore the behavior of metal films with different parameters with the help of CNF in the coming year. This information will help us to improve sample design and how best to reduce noise due to sample dielectric fluctuations without reducing our ability to detect sample spins.

References:

[1] Ariyaratne, A. et al.; Nat Commun, 2018, 9, 2406.

Investigation of Area Selective Atomic Layer Deposition with Microreactor and *in situ* Surface Analysis

CNF Project Number: 1239-04

Principal Investigator(s): James R. Engstrom

User(s): Taewon Suh, Colleen Lawlor

Affiliation(s): Robert Frederick Smith School of Chemical and Biomolecular Engineering, Cornell University

Primary Source(s) of Research Funding: Semiconductor Research Corporation

Contact: jre7@cornell.edu, ts695@cornell.edu, ccl233@cornell.edu

Website: http://engstromgroup.cbe.cornell.edu

Primary CNF Tools Used: Acid hood, atomic layer deposition (ALD)

Abstract:

Atomic layer deposition (ALD) is a technique capable of precise control of film thickness and conformal film growth due to self-limiting nature of the precursors. Engstrom research group (ERG) has built a microreactor through which reactants of ALD are delivered and confined in a small region for deposition. This microreactor is coupled to an ultra high vacuum (UHV) chamber for surface characterization such that the deposited film is transferred *in vacuo*, without an air break, to the analysis chamber. In addition to the two reactants used in conventional ALD:ALD precursor and co-reactant, a third species called "co-adsorbate" is introduced for possible area selective deposition to act as a site-blocking layer.

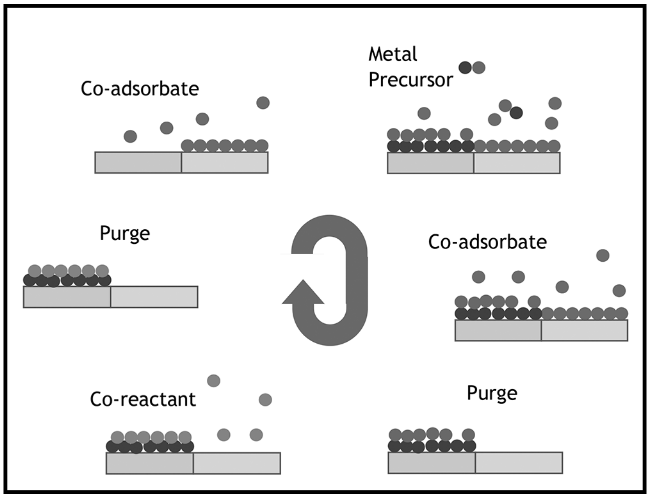

Figure 1: Schematic of an ALD cycle with co-adsorbate molecules.

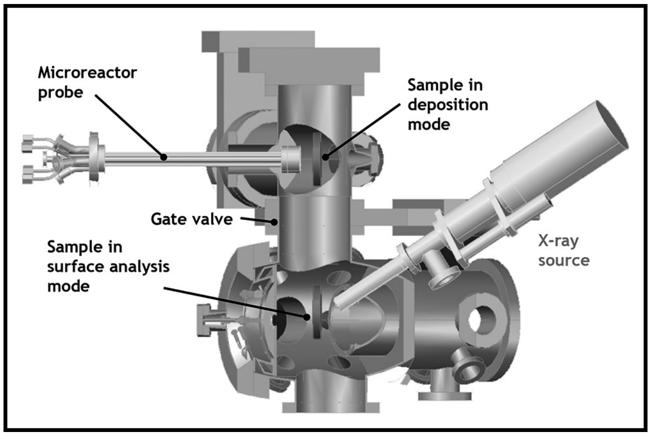

Figure 2: CAD rendering of the microreactor and UHV surface analysis chamber.

Summary of Research:

In continuous downscaling of semiconductor devices, ALD has emerged as a potential approach capable of meeting required criteria of next generation technologies. The self-limiting nature of ALD precursors brings about two major advantages unique to the technique: precise control of thickness of deposited film and conformal growth [1]. ALD is sequential binary gas-phase reaction separated by purge steps to prevent any unwanted parasitic reactions between the precursor and co-reactant. ERG takes this deposition technique a step further to study fundamental mechanisms involved in potential area-selective ALD. Co-adsorbate molecules are introduced within a conventional cycle of ALD: before, during, and after precursor pulse as in Figure 1, to investigate how this third species potentially allows for area selective deposition. The deposited film is transferred *in vacuo* to and characterized in a UHV chamber coupled with the microreactor using XPS.

The thickness of deposited film (~ a few nm) is often in the range that is most effectively probed with surface-sensitive characterization techniques that require UHV, $p < 10^{-9}$ Torr. Conventional ALD is typically conducted at low to medium vacuum conditions ($p \sim 10^{-3}$-10^{-2} Torr), thus in most cases UHV based analysis of the deposited thin films occurs in a separate chamber, requiring an air break that may significantly alter the surface composition, oxidation state, structure of the deposited film, and/or underlying substrate. Avoiding this air break is critical for fundamental studies of the growth of ultrathin films, particularly in the early stages. Figure 2 describes how a sample is exposed to precursors at the upper stage and transferred down to the lower stage of the chamber without exposure to air for post-deposition characterization.

In this report, we investigate a mechanism that can possibly achieve area-selective deposition with ALD by employing co-adsorbate molecules. Two substrates of different composition are used as initial surfaces: chemical oxide and metallic copper. Substrate preparation for the dielectric is conducted in the acid hood of CNF at Cornell University. This wet chemical etch includes submerging Si <100> wafer in buffered oxide etch (BOE) (6:1) for two minutes that produces hydrogen-terminated Si, confirmed by hydrophobicity of the surface. The substrate is then immersed in nanostrip for 15 minutes, which generates hydroxyl group termination with a known density of ~ 5×10^{-14} OH/cm^{-2} [2]. This cycle of removing native oxide and generating chemical oxide is repeated twice. OH-terminated SiO_2 and copper substrates are loaded into the vacuum chamber within a sample holder which allows simultaneous exposure of substrates to reactants such that gas-surface reactions will occur under identical+ experimental conditions.

In area-selective ALD experiments, substrates are annealed to substrate temperature of 180°C for an hour prior to exposure. Then co-adsorbate species, unsaturated hydrocarbon in this report, is introduced to surfaces to form site-blocking layer to prevent incoming ALD precursor from adsorbing on non-growth surfaces. The co-adsorbate molecules are present at relatively high ratio compared to ALD precursor before, during, and after the precursor pulse to ensure excess co-adsorbate molecules are present for competitive adsorption. After purge of the precursor and co-adsorbate, pulse and purge of co-reactant occurs, just like the second half cycle in conventional ALD. Deposited metal oxide films are characterized with *in situ* x-ray photoelectron spectroscopy (XPS) using several parameters: photoionization cross section, inelastic mean free path, and kinetic energy, etc. [3]. The absolute atomic density of metal atom is calculated using calibration of semi-infinite Au film and methods described elsewhere [4].

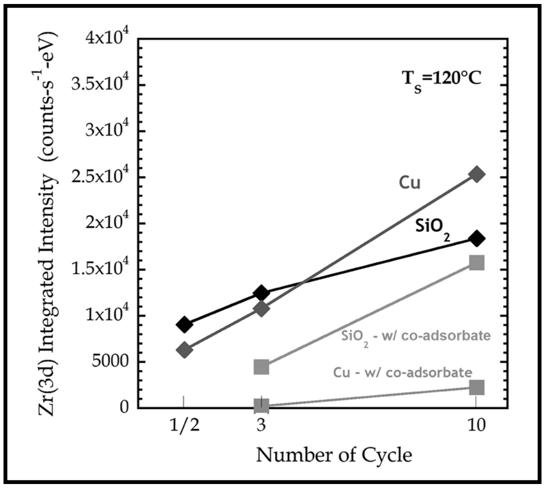

Figure 3: Sample holder capable of holding two coupon samples.

Results from preliminary AS-ALD experiments with an unsaturated hydrocarbon as the co-adsorbate species are summarized in Figure 3. The top two curves represent the integrated intensity of Zr(3d) detected in ½, 3, and 10 ALD cycles of Zr-containing precursor with an oxidant. As expected for an ALD process, the amount of transition metal within the deposited thin film is linearly proportional to the number of cycles. Density functional theory (DFT) calculations demonstrate that the co-adsorbate species has stronger affinity towards Cu than SiO_2. Experimental results show good correlation with the theoretical calculations; in Figure 3, the two bottom curves represent the amount of Zr(3d) detected on SiO_2 and Cu from 3 and 10 ALD cycles in presence of the co-adsorbate.

In the three-cycle experiment with the co-adsorbate, complete inhibition of Zr adsorption is obtained, most likely due to competitive adsorption between the co-adsorbate and ALD precursor for surface active sites. In the ten-cycle experiment, some Zr(3d) is detected, but the amount of Zr on SiO_2 compared to Zr on Cu is greater by approximately a factor of 10.

References:

[1] S. M. George, "Atomic layer deposition: An overview," Chem. Rev., vol. 110, pp. 111-131, 2010.

[2] L. T. Zhuravlev, "Concentration of hydroxyl groups on the surface of amorphous silicas," Langmuir, vol. 3, no. 3, pp. 316-318, 1987.

[3] J. H. Scofield, "Hartree-Slater subshell photoionization cross-sections at 1254 and 1487 eV," J. Electron Spectros. Relat. Phenomena, vol. 8, no. 2, pp. 129-137, 1976.

[4] K. J. Hughes and J. R. Engstrom, "Interfacial organic layers: Tailored surface chemistry for nucleation and growth," J. Vac. Sci. Technol. A Vacuum, Surfaces, Film., vol. 28, no. 5, p. 1033, 2010.

Thin Film, Laser-Etched Sorbent Sheets for Spatially Resolved and High Throughput Analysis of Volatiles

CNF Project Number: 2513-16

Principal Investigator(s): Gavin Sacks

User(s): Jessica Rafson, Madeleine Bee

Affiliation(s): Department of Food Science, Cornell University

Primary Source(s) of Research Funding: United States Department of Agriculture, National Institute of Food and Agriculture (USDA-NIFA) Award #2017-67007-25940

Contract: gls9@cornell.edu, myb8@cornell.edu, jr2255@cornell.edu

Website: http://blogs.cornell.edu/winechemistry/

Primary CNF Tools Used: VersaLaser engraver/cutter tool

Abstract:

The analysis of trace-level volatiles responsible for odor of foods, beverages, and other systems is challenging because of their low concentrations, often down to part-per-trillion (nanogram-per-liter) levels. Because of this, trace volatile analyses often require pre-concentration and extraction steps, followed by lengthy analysis on gas chromatography — mass spectrometry (GC-MS). Often, analyses require 30 min per sample. Using tools available through the Cornell NanoScale Facility (CNF), we have prepared etched sorbents sheets. These sheets can be used to extract multiple samples in parallel, either from multiwell plates or other planar surfaces. The etched geometry of the sheets facilitates their direct coupling with mass spectrometers, and allows for very rapid analyses of trace volatiles — up to 24 samples in 17 min, or over 10-fold faster than conventional approaches. Additionally, because the extraction step preserves the spatial distribution of volatiles, it can also be used for imaging analyses of volatiles.

Summary of Research:

The odors associated with common foods, beverages, and fragrances are due to range of odorants, many present at concentrations as low as a part-per-trillion (nanogram-per-liter, or ng/L). Because of these low concentrations, analysis of these trace volatiles often requires initial steps to concentrate them and remove interferences, followed by analysis by techniques like gas chromatography — mass spectrometry (GC-MS).

GC-MS analyses often require 30 min per sample and represent a common bottleneck in characterization of large numbers of samples. So-called "ambient-ionization" — MS techniques like direct analysis in real time (DART) — are much faster than GC-MS, but coupling automated extraction approaches to DART-MS has not been straightforward. To overcome this, our group developed an approach called Solid Phase Mesh Enhanced Sorption from Headspace (SPMESH), which is readily coupled to DART-MS, as shown in Figure 1.

Our group used the VersaLaser cutting tool at the CNF to generate mesh patterns on poly(dimethylsiloxane) (PDMS) sheets shown in Figure 2. We could then position the sheets over multiwell plates pre-loaded with samples, e.g. macerated grapes. The silicone sheets then absorbed the volatiles in the headspace above each well in parallel. Following extraction, the SPMESH sheet with extracted volatiles is then transferred to an automated positioning stage. Using three representative odorants, we were able to use SPMESH-DART-MS to analyze 24 samples in 17 min with detection limits in the ng/L range, shown in Figure 3 [1]. We also showed that the approach had excellent day-over-day repeatability (< 25% in signal over two weeks).

In a follow-up study [2], we reported that SPMESH absorption could also be performed from headspace of other planar surfaces, including samples spotted on thin-layer chromatography (TLC) plates. The use of TLC plates greatly enhanced the extraction rate, such that extraction only required 2-3 min to reach equilibrium. We also demonstrated that spatial distribution of volatiles could be preserved during imaging, allowing SPMESH to be used for imaging of volatiles from a surface, as shown in Figure 4.

In summary, laser-etched SPMESH sheets can be used for both high-throughput extraction and analysis of trace volatiles, as well as imaging of the spatial distribution of volatiles.

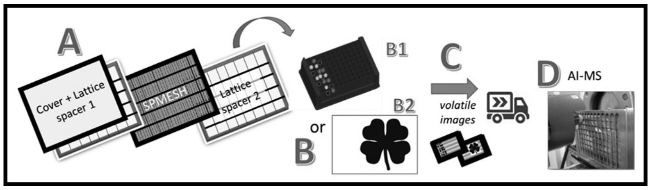

Figure 1: Overview of new approach to volatile analyses. Sorbent coated laser-etched meshes (SPMESH, A), are situated between inert lattice spacers, and positioned over welled plates for high-throughput quantification (B1) or over an intact sample for imaging analyses (B2). Following parallel headspace extraction to create volatile images (C), the SPMESH sheet can be rapidly analyzed by ambient ionization - mass spectrometry (AI-MS, e.g., DART-MS (D)).

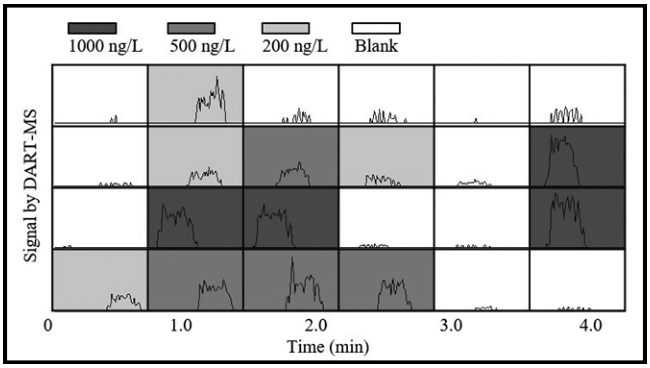

Figure 3: High-throughput SPMESH-DART-MS analyses of a trace level volatile (IBMP, "green pepper aroma") from a multi-well plate. Each cell represents a sample on a 24-well plate, containing 0-1000 ng/L IBMP.

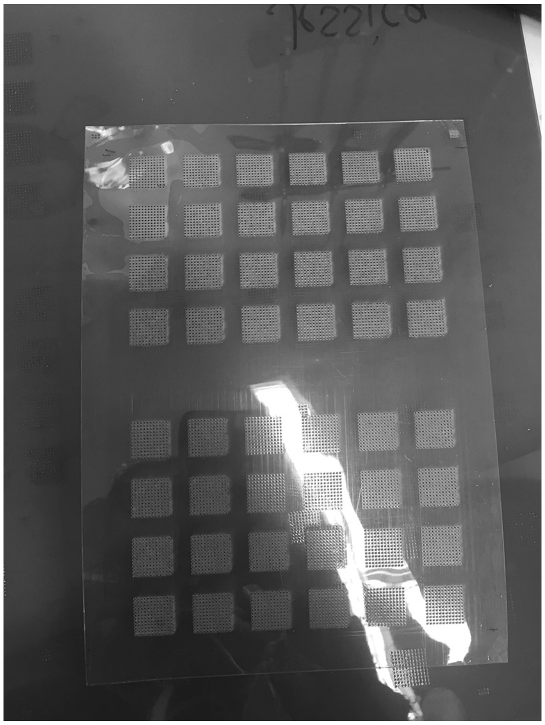

Figure 2: Etched silicone SPMESH sheet produced at the CNF. The grid size is 0.5 mm × 0.5 mm.

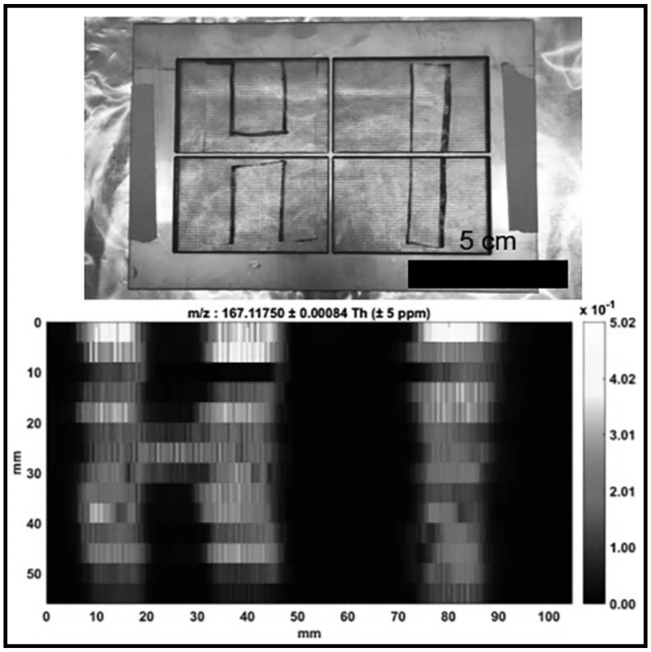

Figure 4: Spatially resolved image (bottom) of a volatile deposited on a polyethylene film (top) using SPMESH-DART-MS.

References:

[1] Bee MY, Jastrzembski JA and Sacks GL. Parallel headspace extraction onto etched sorbent sheets prior to ambient-ionization mass spectrometry for automated, trace-level volatile analyses. Analytical Chemistry. 90, pp. 13806-13813. https://pubs.acs.org/doi/10.1021/acs.analchem.8b04465 (2018).

[2] Rafson J, Bee MY, Sacks GL. Spatially resolved headspace extractions of trace-level volatiles from planar surfaces for high-throughput quantitation and mass spectral imaging. Journal of Agricultural and Food Chemistry. https://pubs.acs.org/doi/10.1021/acs.jafc.9b01091 (2019).

Fabrication of Graphene Microelectrodes

CNF Project Number: 2618-17
Principal Investigator(s): Prof. Héctor D. Abruña
User(s): Dr. Matej Velický

Affiliation(s): Department of Chemistry and Chemical Biology, Cornell University

Primary Source(s) of Research Funding: European Union/European Commission

Contact: hda1@cornell.edu, mv337@cornell.edu
Website: https://abruna.chem.cornell.edu

Primary CNF Tools Used: Anatech resist strip, Nikon L200 eclipse microscope, Heidelberg mask writer DWL2000, ABM contact aligner, SC4500 odd-hour evaporator, YES vapor prime oven

Abstract:

We present a method of graphene microelectrode fabrication, which we designed to be able to study the electrochemical properties and applicability of graphene in energy storage, sensing, and electrocatalysis. The fabrication scheme consists of mechanical exfoliation of graphene/graphite crystals, photolithographic pattering of their surface, and metal deposition of electrical contacts.

Summary of Research:

The electrochemistry of two-dimensional (2D) materials such as graphene has been of significant interest to researchers hoping to apply these materials in energy storage, sensing, and electrocatalysis [1]. However, a limited understanding of the fundamental electrochemical properties of graphene has hindered the recent progress, mostly due to lack of well-defined single-crystal graphene samples. Our aim was to fabricate microscale opening within an insulating layer of a polymer in order to study the electrochemical properties of single-crystal graphene/graphite microelectrodes. To that end, we exfoliated bulk graphite onto an insulating substrate and used polymer-based photolithography and metal deposition to create an electrical contact to graphene/graphite and to fabricate the microelectrode opening over the material.

First step in the fabrication process is the mechanical exfoliation of bulk graphite onto anoxidized silicon wafer (SiO_2/Si). The wafers are sonicated in acetone and isopropanol (IPA) in order to remove surface contamination. To maximize the adhesion between the graphite and the wafer, the latter is cleaned by plasma ashing in the Anatech resist strip (at 900 W for 5 min), immediately prior to the graphite exfoliation. The tape use for exfoliation is peeled away, leaving some graphite/graphene crystals on the wafer surface. Examination under the Nikon L200 eclipse microscope reveals crystal of different thickness, readily identified by their optical contrast, as shown in Figure 1.

We then designed and wrote a quartz/chrome photomask (courtesy of Alejandro J. Cortese, McEuen group) using the Heidelberg mask writer DWL2000, to be used with our two-step photolithographic process. Poly(methyl methacrylate) (PMMA) (950K 4% in anisole) was used as the photoresist polymer material for both steps, using the 220 nm mirror, 60 min exposure, and methylisobutyl ketone/IPA (1:3) developer. First, the mask was manually aligned to a selected graphene/graphite crystal and exposed using the ABM contact aligner. This was done in a way such that a window in the PMMA was created, exposing a small portion of the crystal as shown in Figure 2.

Next, the SC4500 odd-hour evaporator was used to deposit a layer of 7 nm Cr and 50 nm Au. The PMMA and top-surface Au/Crwere then removed by a lift-off procedure in acetone (assisted by a methyl methacrylate undercut layer). This resulted in the exposed portion of the crystal in contact with the Au/Cr layer, as shown in Figure 3.

In the second photolithographic step, another PMMA layer was used to cover the entire wafer, another pattern on the mask was aligned to the alignment marks from the previous metal deposition step and exposed using the ABM contact aligner. This resulted in a microelectrode disk opening in the PMMA, exposing the graphene/graphite surface in the final device shown in Figure 4. We then contacted the Au layer to metal wire and erected

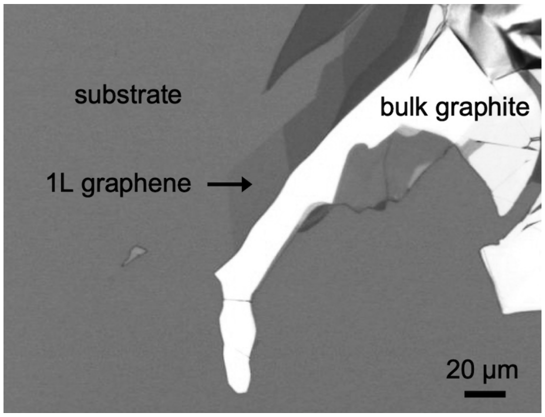

Figure 1: Optical image of graphene/graphite crystals exfoliated on 290 nm SiO_2/Si substrate.

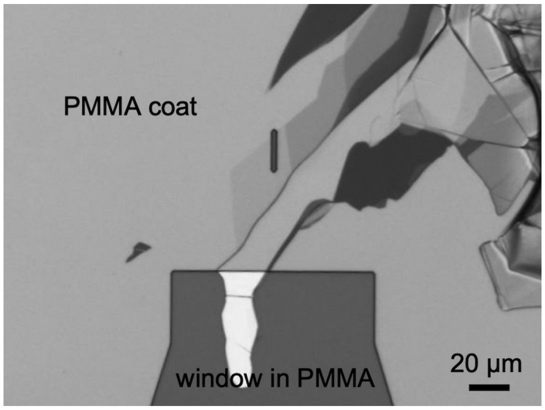

Figure 2: Optical image showing the first photolithographic step with a window in the PMMA exposing apart of the graphite crystal.

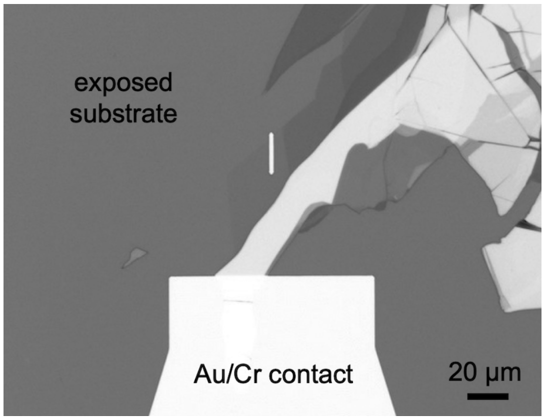

Figure 3: Optical image showing the deposited Au/Cr layer contacting the graphite crystal.

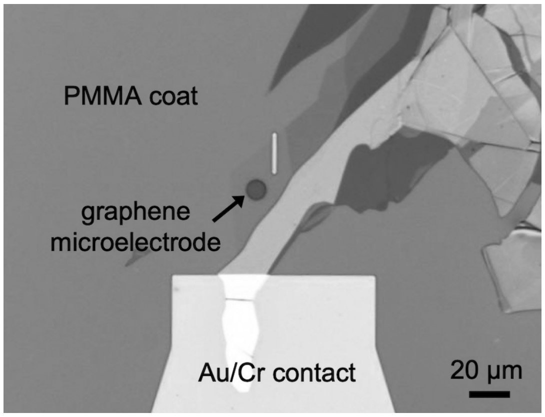

Figure 4: Optical image showing the final device with a 10 µm diameter opening in PMMA exposing a monolayer graphene crystal microelectrode.

an electrochemical cell around this opening made of a several-mm thick polydimethylsiloxane (PDMS), which has previously been set over a silicon wafer surface primed with hexamethyldisilazane using the YES Vapor Prime Oven. The PDMS "pool" has been filled with the liquid solution of interest in order to carry out the electrochemical experiments.

To date, we have not been able to achieve satisfying electrochemical behavior of our devices. Specifically, we either observed no current upon application of voltage or current-voltage characteristics significantly deviating from the behavior expected for the device geometry. We suspect that there are several factors contribute to this discrepancy, namely contamination of the microelectrode from the photolithographic process and either pinholes in PMMA or poor adhesion between the PMMA and the SiO_2/Si substrate, resulting in the liquid "creeping" between the two.

In summary, we succeeded in designing a fabrication scheme, which can produce graphene/graphite electrodes of diameters between 5-100 µm. We currently work towards resolving the aforementioned issues affecting the electrochemical measurement of these devices. We envisage that once these technical obstacles are resolved, we will able to study some of the fundamental relationships, namely the effect of the electric field upon the electron transfer rate between a graphene electrode and a redox molecule in solution. Such fundamental insights will facilitate exploration of graphene and other 2D materials in the electrochemical energy storage/conversion, sensing, and electrocatalysis.

References:

[1] Velick., M. and Toth, P. S. From Two-Dimensional Materials to Their Heterostructures: An Electrochemist's Perspective. Appl. Mater. Today 2017, 8, 68-103.

Small Molecule Photoresists for EUV Lithography

CNF Project Number: 2656-18

Principal Investigator(s): Emmanuel Giannelis, Christopher Kemper Ober

User(s): Wenyang Pan

Affiliation(s): Materials Science and Engineering, Cornell University

Primary Source(s) of Research Funding: JSR

Contact: epg2@cornell.edu, cko3@cornell.edu, wp222@cornell.edu

Primary CNF Tools Used: ASML 300C DUV stepper, ABM contact aligner, Zeiss Ultra SEM

Abstract:

We are developing novel small molecule photoresists that are compatible with the state-of-art extreme ultraviolet (EUV) lithography, and represent under 10 nm resolution.

Summary of Research:

In the Giannelis group and the Ober group, we are developing a class of novel photoresists that are small enough for the current EUV lithography [1,2]. These photoresists are small molecules that crosslink upon exposure under DUV or EUV.

We normally develop the chemistry in our labs at MSE, Cornell. Once we have got a new recipe, we expose our thin film using the contact aligner and DUV stepper at certain wavelengths in CNF. We also rely heavily on CNF SEM to check our resolution. Certain chemistry would also be evaluated for e-beam lithography, which is performed by another colleague in Ober group.

References:

[1] Sakai, Kazunori, et al. “Development of metal organic cluster EUV photoresists.” Advances in Patterning Materials and Processes XXXVI. Vol. 10960. International Society for Optics and Photonics, 2019.

[2] Sakai, Kazunori, et al. “Metal organic cluster photoresists: new metal oxide systems.” Advanced Etch Technology for Nanopatterning VIII. Vol. 10963. International Society for Optics and Photonics, 2019.

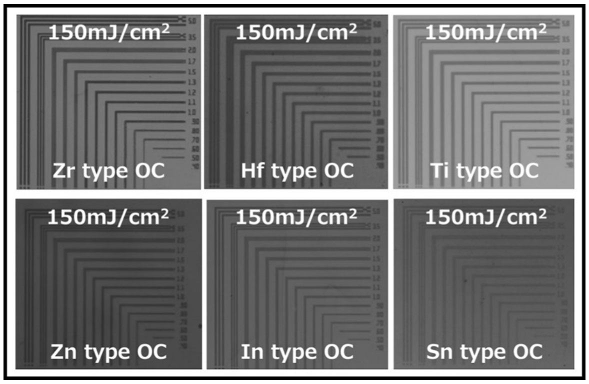

Figure 1: Micron-scale patterning results from contact aligner in CNF, of several resists.

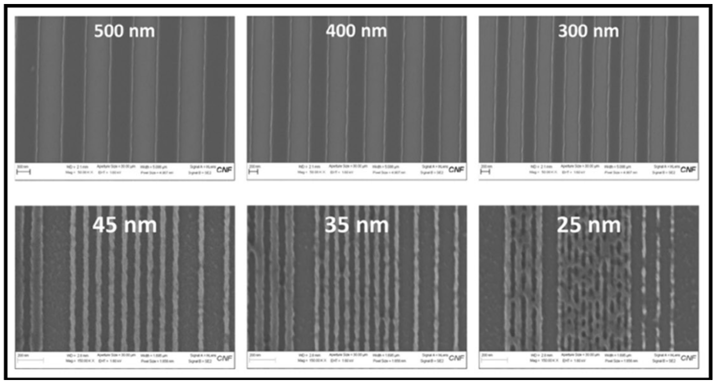

Figure 2: DUV exposure (upper), in CNF, and further evaluation using finer masks (lower) exposure one organic cluster resist.